

# Nanodiamond-Embedded Microfilm Devices for Localized Chemotherapeutic Elution

Robert Lam,<sup>†</sup> Mark Chen,<sup>†</sup> Erik Pierstorff,<sup>†</sup> Houjin Huang,<sup>†</sup> Eiji Osawa,<sup>‡</sup> and Dean Ho<sup>†,§,\*</sup>

<sup>†</sup>Departments of Biomedical and Mechanical Engineering, Robert R. McCormick School of Engineering and Applied Science, Northwestern University, Evanston, Illinois 60208, <sup>‡</sup>Nanocarbon Research Institute, Ltd., Asama Research Extension Center, Shinshu University, 3-15-1 Tokita, Ueda, Nagano 386-8567, Japan, and <sup>§</sup>Robert H. Lurie Comprehensive Cancer Center of Northwestern University, Chicago, Illinois 60611

Numerous synthetic and natural nanoscale carriers have been developed and investigated for modulating therapeutic release. These include, but are not limited to polymer–protein conjugates, liposomes, micelles, dendrimers, polyelectrolyte films, copolypeptides, carbon nanotubes, carbon nanohorns and variants of the above.<sup>1–8</sup>

Nanodiamonds (NDs) in particular possess several characteristics including surface functionalization capabilities, biocompatibility, and versatile deposition and processing mechanisms that make them suitable for advanced drug delivery.<sup>9–17</sup> NDs have formerly been physically immobilized and functionalized in various ways in order to bind with cytochrome *c*, DNA, antibodies, and various protein antigens.<sup>10,12,18–22</sup> In addition, we have previously demonstrated the ability to adsorb 2–8 nm diameter ND powders with the apoptosis-inducing chemotherapeutic agent, DOX, and anti-inflammatory immunosuppressant glucocorticoid, dexamethasone for drug delivery.<sup>23,24</sup> Because of their high surface area to volume ratio, up to 450 m<sup>2</sup> g<sup>-1</sup>, and noninvasive dimensions, extremely high loading capacities of therapeutic are achievable.<sup>25</sup> In addition, we have demonstrated the capability of ND interfacing with virtually any therapeutic molecule *via* physical interactions due to tailorable surface properties and compositions.<sup>24</sup> With highly ordered aspect ratios near unity, NDs have been shown to be biologically stable, allowing them to preclude adverse cellular stress and inflammatory reactions.<sup>26,27</sup> Several reports have confirmed the inherently amenable biological performance of suspended NDs when interacting with cells.<sup>16,17,23,24,26–28</sup> Particularly,

**ABSTRACT** Nanodiamonds (NDs) of 2–8 nm diameters physically bound with the chemotherapeutic agent doxorubicin hydrochloride (DOX) were embedded within a parylene C polymer microfilm through a facile and scalable process. The microfilm architecture consists of DOX-ND conjugates sandwiched between a base and thin variable layer of parylene C which allows for modulation of release. Successive layers of parylene and the DOX-ND conjugates were characterized through atomic force microscopy (AFM) images and drug release assays. Elution rates were tested separately over a period of 8 days and up to one month in order to illustrate the release characteristics of the microfilms. The microfilms displayed the stable and continuous slow-release of drug for at least one month due to the powerful sequestration abilities of the DOX-ND complex and the release-modulating nature of the thin parylene layer. Since the fabrication process is devoid of any destructive steps, the DOX-ND conjugates are unaffected and unaltered. A DNA fragmentation assay was performed to illustrate this retained activity of DOX under biological conditions. Specifically, in this work we have conferred the ability to tangibly manipulate the NDs in a polymer-packaged microfilm format for directed placement over diseased areas. By harnessing the innate ND benefits in a biostable patch platform, extended targeted and controlled release, possibly relevant toward conditions such as cancer, viral infection, and inflammation, where complementary alternatives to systemic drug release enabled by the microfilm devices, can allow for enhanced treatment efficacy.

**KEYWORDS:** nanodiamonds · nanomedicine · nanomaterials · slow-release · drug delivery

the general cellular viability, morphology, and mitochondrial membrane is maintained among various cell types when incubated with suspended NDs.<sup>26,28</sup> As such, with appropriate manipulation of drug elution parameters in conjunction with proper selection of material matrices, NDs serve as promising platforms for sustained and localized therapeutic release.

Previous studies concerning covalently modified ND films fabricated *via* chemical vapor deposition (CVD) with various biological entities have provided exciting prospects for biosensing applications but are nonetheless difficult to implant because of their rigidity.<sup>29,30</sup> We have also previously demonstrated the application of self-assembled nanodiamond laminated structures *via* layer-by-layer processing, an

\*Address correspondence to d-ho@northwestern.edu.

Received for review July 24, 2008 and accepted September 15, 2008.

Published online October 2, 2008. 10.1021/nn800465x CCC: \$40.75

© 2008 American Chemical Society

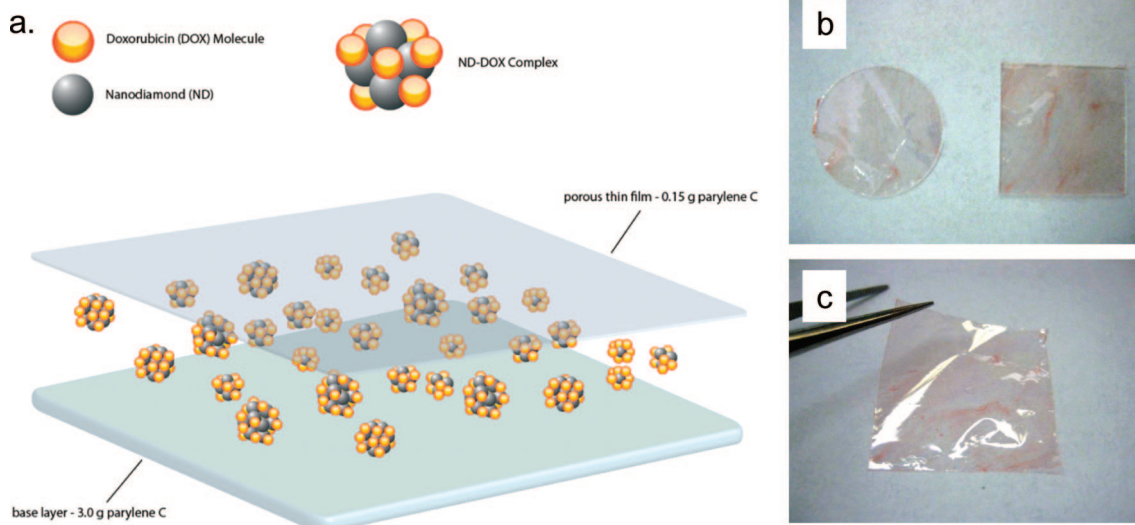


**Figure 1.** (a) Illustrated schematic of hybrid film patch. NDs and DOX molecules bound through physical interactions in various configurations are deposited atop a base layer of parylene. A final layer of parylene film is then deposited for additional elution control. (b) Hybrid films with a 10 g base layer of varied size and shapes. (c) The patch exhibits innate flexibility and a thin physical profile.

important precursor for local release in the form of a coating.<sup>24</sup>

In this work, we describe the development of a scalably fabricated flexible microfilm patch device which harnesses the release activity of nanodiamonds for significantly extended drug release capabilities in a localized format. These nanodiamond-embedded polymeric microfilms utilize the aforementioned benefits associated with NDs with minimal to no impact upon the dimensions of the device, thereby realizing a high-load capacity system that is inherently noninvasive architecturally. Because of the innate biostability of the parylene polymer platform that was utilized for encapsulation, this technology can serve as a foundation for ultralong term drug elution which can address the need for a broad range of medical disorders including cancer, inflammation, and viral infection in a tangible form allowing directed device placement toward virtually any specified location.

Parylene C, a material with well-documented biocompatibility and FDA-approval, is used as a flexible and robust framework and nanodiamond packaging agent for microfilm fabrication.<sup>31,32</sup> Parylene surfaces have been utilized in several medical applications because of their highly conformal nature, biostability, and inertness under physiological conditions with no known adverse biological degradation events.<sup>31,33–36</sup>

The hybrid film consists of DOX–ND conjugates sandwiched between a thick hermetic base and thin permeable layer of parylene C (Figure 1a). NDs efficiently sequester DOX, and can be released gradually upon appropriate stimuli, that is, DOX concentration gradients and acidic pH conditions, which have been shown to be indicative of cancerous cells. A permeable top layer of parylene C additionally acts as a physical

barrier that further limits and modulates elution. This microfilm architecture can address a broad range of medical conditions including difficulties involving tumor heterogeneity, blood circulation, and unsustainable controlled release over a prolonged period of time.<sup>37</sup> Therefore, the ND-parylene hybrids possess particular significance and relevance toward oncological and anti-inflammatory translation through functionalization of different disease specific drugs. The biocompatible properties, customization and localization capacity of the flexible parylene C encapsulated DOX–ND hybrid film (Figure 1b,c) addresses several of these difficulties and offers a promising method and avenue for future drug delivery schemes.

## RESULTS AND DISCUSSION

This work demonstrated the fabrication of an ND-based device by embedding drug-ND matrices within a parylene C microfilm. While we have demonstrated the foundational ability to physically adsorb therapeutics onto ND surfaces for particle and self-assembled interface-driven release, the microfilm device transitions the ND from a fundamental material toward systemic fabrication.<sup>23,24</sup> This microfilm has conferred to the ND matrix the tangibility for directed placement and localized chemotherapeutic release. Additionally, device performance harnesses the slow-desorption and sustained delivery properties of the NDs toward biostable cancer cell therapy.

For elution and biological assay studies, a conformal and impenetrable base layer of parylene C was deposited atop precut glass slides. Within the parylene deposition machine, the parylene C dimer (*di-parylylene*) is pyrolyzed into monomer form (*para-parylylene*) and then deposited at room temperature in a

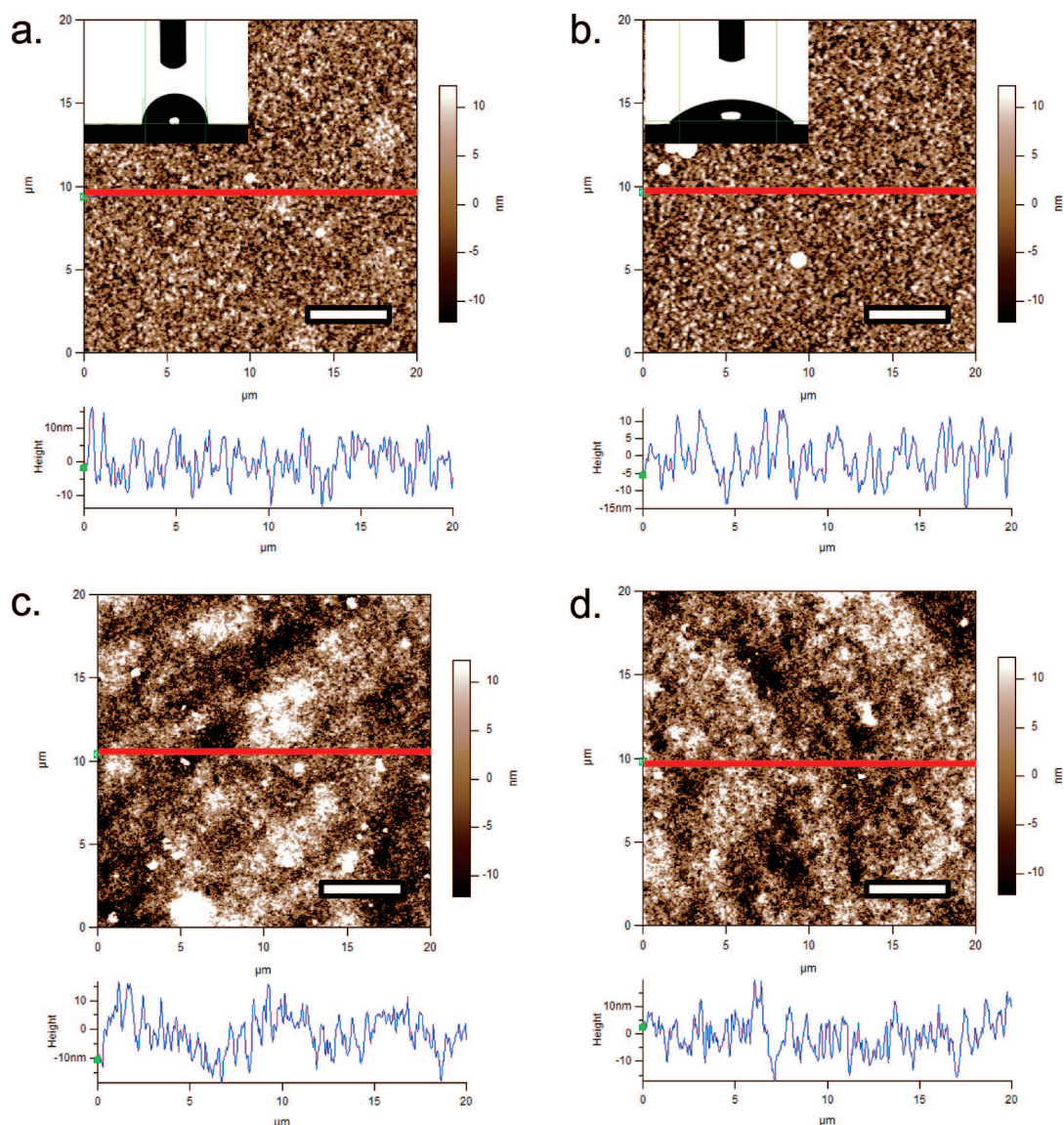


**Figure 2.** (a, b) Atomic force microscope (AFM) images reveal the coarse grained polymer structure of native and plasma treated parylene C, with an rms roughness of 6.245 and 9.291 nm, respectively. The rms roughness values were obtained through Asylum's MFP-3D/Igor Pro software. Insets: static contact angle measurements exhibit the hydrophilicity transformation associated with plasma treatment. (c) DOX–NDs were deposited on a plasma treated layer of parylene C. The images portray nanoscale features that form *via* parylene coating of the DOX–ND conjugates, possibly due to the general roughness of the underlying parylene or ND aggregation. (d) DOX–NDs were covered with an additional thin layer of parylene C. General structure and conformation of the underlying DOX–NDs were unaffected by the thin film of parylene C deposition; scale bars = 5  $\mu\text{m}$ .

vacuum, where the monomers spontaneously form polymers.<sup>35,38</sup> Since this process takes place under ambient conditions, the functionality and structure of the DOX–ND conjugates are not harmed or inhibited.

The base layer exists as a flexible foundation upon which an implantable patch can be constructed and simultaneously provides an impermeable and pinhole-free platform for unidirectional drug-elution. As newly deposited parylene is hydrophobic as elucidated by fundamental surface nanostructure studies (Figure 2a),<sup>39</sup> additional surface processing was performed to enhance drug deposition uniformity and elution. As such, the parylene layers were oxidized *via* oxygen plasma treatment, which has been shown to increase

surface roughness while adding  $\text{CO}_3^-$  and carbonyl ( $\text{C}=\text{O}$ ) groups, effectively creating a hydrophilic surface (Figure 2b).<sup>40</sup> Oxidation of parylene C surfaces have been shown to be stably hydrophilic after treatment, while increasing the level of cell adhesion.<sup>36</sup> For elution experiments, appropriate amounts of a DOX–ND solution composed of a 4:1 ratio of NDs and DOX of concentrations 330 and 66  $\mu\text{g}/\text{mL}$ , respectively, was then added to the base layers *via* solvent-evaporation at room temperature to produce a final concentration of 6.6  $\mu\text{g}/\text{mL}$  in solution (Figure 2c).

A second ultrathin parylene C layer of patchy porosity was then deposited as an elution limiting element (Figure 2d). At diminutive parylene dimer loads, film

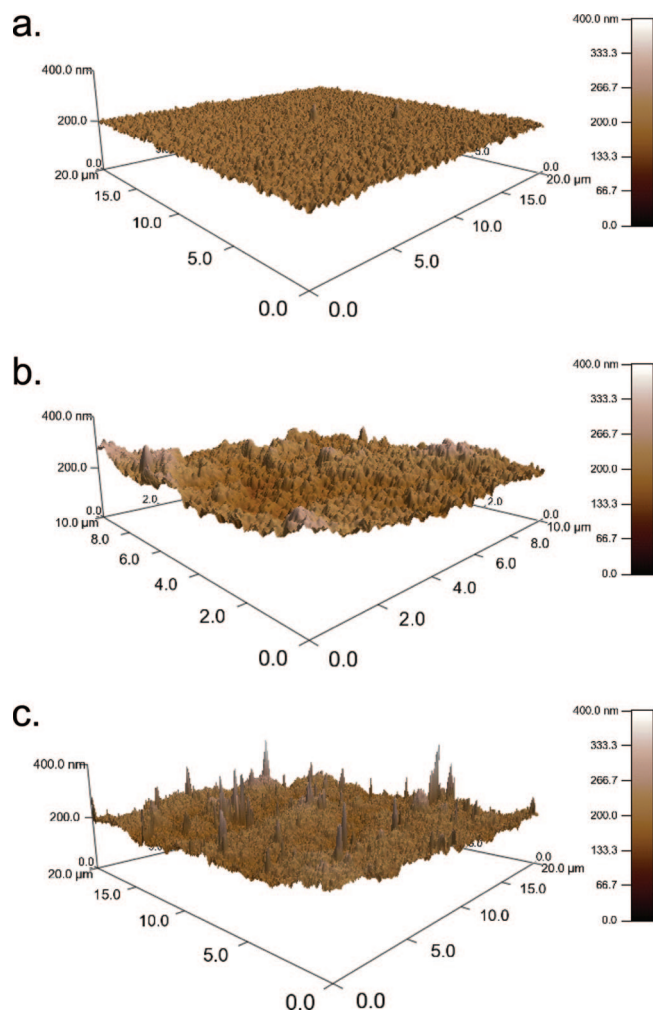


**Figure 3.** 3-d AFM representations of the (a) 1st layer, oxidized parylene C base; (b) 2nd layer, coated DOX–ND deposition on oxidized parylene C base; (c) 3rd layer, top eluting parylene C layer deposited upon DOX–ND conjugates.

deposition cannot be guaranteed to be conformal and pinhole free.<sup>41</sup> Therefore, with smaller dimer masses, the dimensions and amount of pinholes are increased, acting as an adjustable physical barrier for controlled drug release. Furthermore, this additional thin film

provides a structural platform that simultaneously protects the underlying DOX–ND and acts as a base for additional device modifications. We have previously applied this base layer–drug–porous layer configuration toward studies involving DOX and other parylene variations.<sup>42</sup> The final layer of parylene C, with a thickness on the order of 20–50 nm, confirmed through AFM scratch tests (data not shown),<sup>42</sup> was also treated with oxygen plasma.

The topography of each successive layer during processing is exhibited in Figure 3. Of particular importance, the grainy texture of the top eluting parylene layer (Figure 3c) is shown to maintain the structure of the underlying DOX–ND conjugates while simultaneously providing a means for modulating therapeutic release, indicated through slow-release assessment trials.

Slow-release assessments were chosen with DOX due to its easily characterizable absorbance and obtained by immersing samples in nanopure water and placing in a 37 °C and 5% CO<sub>2</sub> incubator to mimic physiological conditions. In addition, the biological function of eluted DOX in a biological environment was examined by identifying apoptosis within a DNA fragmentation assay.

DOX solubilized in water generates an absorbance signal from approximately 375 to 575 nm, with a peak at approximately 480 nm (Figure 4a–b). Absorbance values under 350 nm were not recorded since parylene C is known to absorb strongly at lower wavelengths.

The hybrid films were tested for their initial release profile over the first eight days against a control microfilm of same architecture containing only DOX (Figure 5a). Microfilms containing only DOX eluted the entirety of its drug within the 24 h. In contrast, films that lacked the deposited thin parylene layer eluted the majority of the deposited drug in the first day, while films that contained the layer demonstrated a more controlled and constant release of therapeutic. On the basis of absorbance readings, uncovered DOX–ND complexes eluted at least three times more DOX over the first day

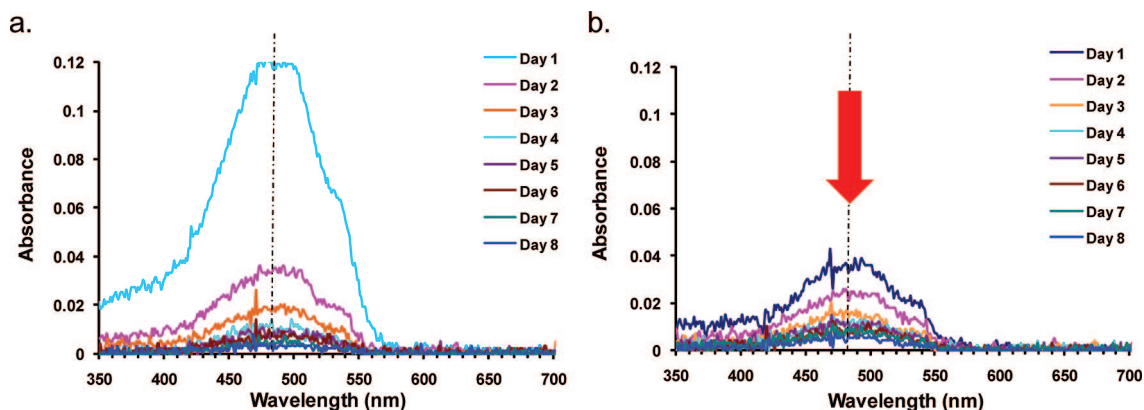


**Figure 4.** Sample of UV–vis spectra of eluate collected at every 24 h interval for uncovered (a) and covered (b) samples. The red arrow in panel b indicates the reduced initial drug elution, especially evident at day 1.

than films with the additional elution control layer, which released drug at a nearly constant rate after 24 h. The muted initial release of the covered films may aid in reducing symptoms associated with spiked levels of drugs that result from direct drug administration. After eight days, there remained a great deal of DOX–ND complexes on both uncovered and covered patches upon visual inspection, possibly due to large aggregations of NDs surrounding a DOX core or physical entrapment onto the uneven coarse oxidized parylene surfaces.<sup>23</sup>

To evaluate the long-term performance of the patch, the experiment was repeated over a month-long period (Figure 5b). An identical initial trend equivalent to the 8-day results was observed. The robustness and stability of the parylene-based patches were confirmed visually throughout the experiment while ongoing trials are examining the continued extension of elution duration to maximize the length of microfilm functionality.

Two important consequences of the initial surge in elution of DOX–ND from the uncovered film affect drug preservation and dosage. First, the decreased ability of the uncovered film in sequestering drug was a direct cause for the increased elution over the first 3 days. In addition, samples were allowed to elute for a period longer than 24 h at specific times to determine extended dosage levels, namely at days 12–16 and 22–29, highlighted in Figure 5b. During the aforementioned periods, covered films eluted a greater total amount of drug than uncovered films, primarily due to the uncovered film's drug reservoir being exhausted at an early stage from its large initial release. Since equal amounts of DOX–ND were coated on both films, the increased elution from the last data point infers the covered hybrid films will elute for a longer period of time than uncovered films.

In addition, the decreased drug preservation of uncovered microfilms resulted in increased initial drug dosage, which can be particularly important during the nascent phases following implantation. An immediate release of drug following implantation has been shown to cause several negative side effects.<sup>43</sup> Therefore, controlled localized elution offers several advantages over conventional systemic drug administration, including the ability of maintaining a desired concentration over long periods of time with a single administration.<sup>3</sup> This continuous elution can alleviate drug loss through blood circulation, extravasation, or other methods of excretion.<sup>44</sup>

Moreover, DOX has poor penetration into tumor tissues, due to low diffusion rates caused by small interstitial spaces and strong intracellular binding.<sup>45</sup> Because of this effect, steep DOX concentration gradients are observed when injected *in vivo*, with the highest concentrations localized near microvessels.<sup>45</sup> A gentler concentration gradient can instead be created with con-

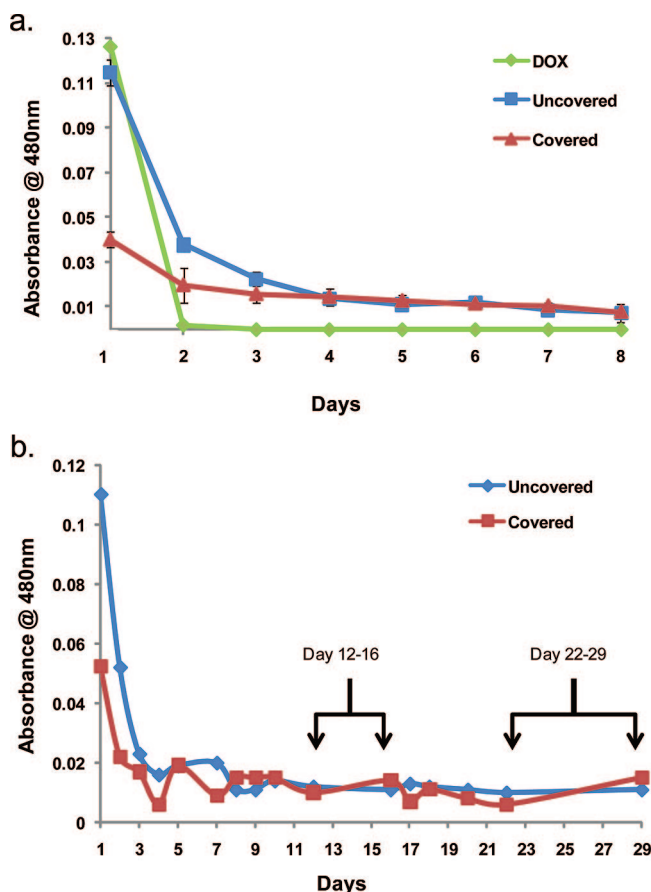
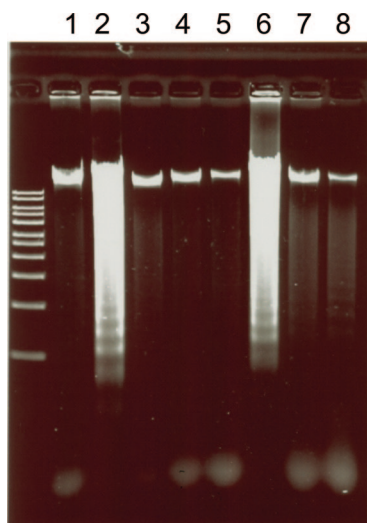


Figure 5. (a) Three initial 8 day trials were performed for a ND-deficient control and uncovered and covered microfilm samples with the optical absorbance measured at 480 nm. (b) A long-term trial where eluate is collected at various time points and optical absorbance is measured at 480 nm. Days 12–16 and 22–29 indicated by arrows are time points representing the specified extended elution period.

tinuous treatment.<sup>45</sup> The ND-parylene microfilm device is envisioned to circumvent these effects since the initial elution of DOX from the hybrid film is gradual and tapered, rather than abrupt and rapidly depleted. Drugs with poor penetration, like DOX, also have low cell-death thresholds, as they only affect cells located at the periphery. Maintained continuous treatment can alleviate this obstacle by eliminating additional layers of cells through lengthened time periods, without supplemental therapies.<sup>46</sup> As an additional benefit, sustained release can prevent oncogenic regrowth between chemotherapy sessions.<sup>46</sup>

To confirm the retained biological activity and sustained elution of DOX mediated by the DOX–ND microfilms, a DNA fragmentation assay was performed (Figure 6). The patterned degradation of DNA that is characteristic of apoptosis appeared as a result of exposure to DOX, and was observed in the gel for the positive control and all samples containing DOX–ND. To show the proper time scale of drug activity, two sets of samples were harvested after 16 (lanes 1–4) and 20 h (lanes 5–8) of growth. Lanes 1:5, 2:6, 3:7, and 4:8 correlate to the negative and positive controls, the uncov-



**Figure 6.** Gel electrophoresis assay of DNA from RAW 264.7 murine macrophages incubated for 16 h (lanes 1–4) and 20 h (lanes 5–8) on glass (lanes 1, 5), parylene with 2.5  $\mu\text{g}/\text{mL}$  of DOX (lanes 2, 6), 33  $\mu\text{g}/\text{mL}$  of DOX–ND on parylene C (lanes 3, 7), and 33  $\mu\text{g}/\text{mL}$  of DOX–ND sandwiched between a base and permeable layer of parylene C (lanes 4, 8). The degrees of banding correlate to different stages of apoptosis induced by DOX incubation.

ered device, and the covered porous device, respectively. DOX–ND microfilm samples were loaded with over 13 times the concentration of DOX compared to the positive control. The ability of DOX–ND complexes to naturally reduce DOX elution rates is seen when comparing lanes 3, 4, 7, and 8 to the 2.5  $\mu\text{g}/\text{mL}$  positive controls. Whereas positive controls prompted rigorous DNA fragmentation, the DOX–ND devices seemed to display a delayed onset of apoptosis, which can reduce the severe side effects that result from a sudden spike in DOX dosage.<sup>47</sup> In addition, the assay attests to the unaffected biological activity native to the DOX–ND complex, even within a biological environment. Moreover, the data substantiates the ability of the device to deliver at least 13 times more therapeutic to a localized spot at a rate of decreased variability. Most importantly, the combined effects of localized delivery and gradual therapeutic elution of a large reservoir of drug offers a safer, yet more enduring, and po-

tent drug delivery device by incorporating other therapeutic agents.

## CONCLUSION

Hybrid parylene-ND-based films were constructed as a flexible, robust, and slow drug-release device intended for implants or as stand-alone devices for specific therapies such as antitumor patches. This device configuration offers a platform on which several therapeutic drug delivery devices can be developed. Hybrid films were capable of releasing a continuous amount of drug for at least a month. We postulate that by altering DOX–ND deposition amounts and the thickness of the permeable parylene layer, dosage amounts and thus, total release times can be calibrated. Since drug release is presumably driven by drug concentration gradients, the patches can be optimized to reduce elution rates should the local therapeutic concentration reach a defined threshold.

Further studies include utilizing layer-by-layer techniques to construct well-ordered ND and drug multilayers on a polymer surface.<sup>24</sup> The flexibility of the critical components in this device, namely the biocompatible structural material, parylene, and the drug sequestering element, NDs, provide exciting prospects involving adjustable and extended timed release with combinatorial drug studies.

Since the DOX–ND complex is highly efficient and regulated for controlled drug release, the patch may serve as a transformative technology for pre- and post-operative therapies to induce localized therapeutic release and tumor apoptosis prior to surgical intervention, or reduce the recurrence of cancer after surgery. Furthermore, the encapsulated NDs may be affixed with fluorescent molecules to serve a dual purpose as an imaging agent for cancer detection or other types of imaging after ND elution. Lastly, the flexibility of this device and scalability of the fabrication process allows the patch to be uniformly coated on any surface including a variety of implants to increase the biocompatibility and functionalities of the coated device.

## MATERIALS AND METHODS

**ND Suspension and Conjugation with DOX.** NDs were conjugated and dispersed according to protocols described in previous studies.<sup>23</sup> Upon ND ultrasonication (100 W, VWR 150D sonicator) for 30 min, DOX and ND solutions were centrifuged together at appropriate concentrations at a 4:1 ratio. Addition of NaCl helped facilitate the process in a more efficient manner.

**Materials and Device Fabrication.** A conformal base layer of parylene C (3 g) was deposited on precut 2.5 cm  $\times$  2.5 cm glass slides with a Specialty Coating Systems (SCS) PDS 2010 Labcoater (SCS, Indianapolis, IN). The parylene layer was oxidized *via* oxygen plasma treatment in a Harrick Plasma Cleaner/Sterilizer (Ithaca, NY) at 100 W for one minute. A DOX–ND solution was then added to the base layer so that the final DOX–ND concentration in solution was 6.6  $\mu\text{g}/\text{mL}$ . Subsequently, solvent evapora-

tion occurred in isolation at room temperature. Following DOX–ND deposition, an ultrathin parylene C (0.15 g) layer was deposited as an elution-limiting and control element. The final layer of parylene C was treated with oxygen plasma at 100 W for one minute. Parylene C was pyrolyzed into a gaseous monomer at 690  $^{\circ}\text{C}$ , and deposited at room temperature under vacuum conditions for all depositions. Control microfilms that lacked NDs were fabricated in the same manner with equal amounts of DOX.

The preceding parameters apply to devices fabricated for spectroscopy studies. The concentration of DOX–ND was adjusted for devices used in the DNA fragmentation assay so that the final DOX–ND concentration in solution was 33  $\mu\text{g}/\text{mL}$ .

**AFM Characterization.** Asylum MFP3D AFM (Santa Barbara, CA) images of the samples were taken to identify the structure and

interaction between proteins. Image dimensions were 20  $\mu\text{m}$   $\times$  20  $\mu\text{m}$ . Contact mode imaging at line scan rates of 0.3 to 0.5 Hz were performed in at room temperature with Olympus TR800PSA 200  $\mu\text{m}$  length silicon nitride cantilevers (Melville, NY).

**Spectroscopic Analysis.** Samples were immersed in nanopure water (2 mL) in six-well plates and placed in an incubator at 37  $^{\circ}\text{C}$  and 5%  $\text{CO}_2$ . At every 24-h interval, samples were transferred to another well to avoid residue contamination while the remaining eluate (2 mL) was collected. A full wavelength scan from 350 to 700 nm was performed on a portion of the eluate (100  $\mu\text{L}$ ) with a Beckman Coulter DU730 Life Science UV/vis spectrophotometer (Fullerton, Ca).

**Contact Angle Measurements.** Static contact angles were measured with DI water (10  $\mu\text{L}$ ) with a Ramé-Hart, Inc. imaging system and autopipetting system (Mountain Lakes, NJ).

**DNA Fragmentation Assay.** RAW 264.7 murine macrophages (ATCC, Manassas, VA) were cultured in Dulbecco's modification of Eagle's medium (Cellgro, Herndon, VA) supplemented with 10% fetal bovine serum (ATCC) and 1% penicillin/streptomycin (Cambrex, East Rutherford, NJ). Cells were grown in an incubator at 37  $^{\circ}\text{C}$  and 5%  $\text{CO}_2$ . The cells were plated on two sets of uncovered and covered devices at  $\sim$ 40% confluence, for 16 h with one set and 20 h with the other to contrast progression of apoptosis over time as a result of DOX-ND elution from the native and porous devices. DOX (2.5  $\mu\text{g}/\text{mL}$ ) served as a positive control for apoptosis, and culture media was a negative control. Cell harvest comprising a PBS wash and subsequent lysis in lysis buffer (500  $\mu\text{L}$ , 10 mM Tris-HCl, pH 8.0, 10 mM EDTA, 1% Triton X-100) for 15 min, 30-min incubations with RNase A (33.3  $\mu\text{g}/\text{mL}$ ) and proteinase K (83.3  $\mu\text{g}/\text{mL}$ ) that occurred at 37  $^{\circ}\text{C}$  followed the buffer treatment, separately. The samples then underwent phenol chloroform extraction, followed by DNA isolation and precipitation in 2-propanol at  $-80^{\circ}\text{C}$  for at least 2 h. After washing with 70% ethanol, the samples were resuspended in water and loaded onto a 0.8% agarose gel in sodium borate buffer, run, and stained with ethidium bromide (Shelton Scientific, Shelton, CT).

**Acknowledgment.** The authors gratefully acknowledge support from a V Foundation for Cancer Research V Scholars Award, National Science Foundation Center for Scalable and Integrated NanoManufacturing (SINAM) Grant DMI-0327077, Wallace H. Coulter Foundation Early Career Award in Translational Research, and National Institutes of Health Grant U54 A1065359.

## REFERENCES AND NOTES

- Peer, D.; Karp, J. M.; Hong, S.; Farokhzad, O. C.; Margalit, R.; Langer, R. Nanocarriers as an Emerging Platform for Cancer Therapy. *Nat. Nanotechnol.* **2007**, *2*, 751–760.
- Volodkin, D.; Arntz, Y.; Schaaf, P.; Moehwald, H.; Voegel, J.-C.; Ball, V. Composite Multilayered Biocompatible Polyelectrolyte Films with Intact Liposomes: Stability and Temperature Triggered Dye Release. *Soft Matter* **2008**, *4*, 122–130.
- Langer, R. New Methods of Drug Delivery. *Science* **1990**, *249*, 1527–1533.
- Wood, K. C.; Chuang, H. F.; Batten, R. D.; Lynn, D. M.; Hammond, P. T. Controlling Interlayer Diffusion to Achieve Sustained, Multiagent Delivery from Layer-by-Layer Thin Films. *Proc. Natl. Acad. Sci. U.S.A.* **2006**, *103*, 10207–10212.
- Wood, K. C.; Boedicker, J. Q.; Lynn, D. M.; Hammond, P. T. Tunable Drug Release from Hydrolytically Degradable Layer-by-Layer Thin Films. *Langmuir* **2005**, *21*, 1603–1609.
- Deming, T. J. Methodologies for Preparation of Synthetic Block Copolypeptides: Materials with Future Promise in Drug Delivery. *Adv. Drug Deliv. Rev.* **2002**, *54*, 1145–1155.
- Lacerda, L.; Bianco, A.; Prato, M.; Kostarelos, K. Carbon Nanotubes as Nanomedicines: From Toxicology to Pharmacology. *Adv. Drug Deliv. Rev.* **2006**, *58*, 1460–1470.
- Zhang, M.; Yudasaka, M.; Ajima, K.; Miyawaki, J.; Iijima, S. Light-Assisted Oxidation of Single-Wall Carbon Nanohorns for Abundant Creation of Oxygenated Groups That Enable Chemical Modifications with Proteins to Enhance Biocompatibility. *ACS Nano* **2007**, *1*, 265–272.
- Gruen, D. M. Nanocrystalline Diamond Films. *Annu. Rev. Mater. Sci.* **1999**, *29*, 211–259.
- Petrov, I. L.; Shenderova, I. L. *Ultra Nanocrystalline Diamond: Synthesis, Properties and Applications*; Shenderova, O. A., Gruen, D. M., Eds.; William Andrew Publishing: New York, 2006; pp 529–550.
- Yeap, W. S.; Tan, Y. Y.; Loh, K. P. Using Detonation Nanodiamond for the Specific Capture of Glycoproteins. *Anal. Chem.* **2008**, *80*, 4659–4665.
- Krüger, A. Hard and Soft: Biofunctionalized Diamond. *Angew. Chem., Int. Ed.* **2006**, *45*, 6426–6427.
- Krüger, A.; Kataoka, F.; Ozawa, M.; Fujino, T.; Suzuki, Y.; Aleksenskii, A. E.; Vul, A. Y.; Ōsawa, E. Unusually Tight Aggregation in Detonation Nanodiamond: Identification and Disintegration. *Carbon* **2005**, *43*, 1722–1730.
- Bondar, V. S.; Puzyr, A. P. Nanodiamonds for Biological Investigations. *Phys. Solid State* **2004**, *46*, 716–719.
- Ozawa, M.; Inaguma, M.; Takahashi, M.; Kataoka, F.; Krüger, A.; Ōsawa, E. Preparation and Behavior of Brownish, Clear Nanodiamond Colloids. *Adv. Mater.* **2007**, *19*, 1201–1206.
- Bakowicz, K.; Mitura, S. Biocompatibility of NCD. *J. Wide Bandgap Mater.* **2002**, *9*, 261–272.
- Bakowicz, K.; Mitura, S. Bioactivity of Diamond. *Proc. IEEE-EMBS Spec. Top. Conf. Mol. Cell. Tiss. Eng.* **2002**, 79–80.
- Huang, L.-C. L.; Chang, H.-C. Adsorption and Immobilization of Cytochrome c on Nanodiamonds. *Langmuir* **2004**, *20*, 5879–5884.
- Ushizawa, K.; Sato, Y.; Mitsumori, T.; Machinami, T.; Ueda, T.; o, T. Covalent Immobilization of DNA on Diamond and its Verification by Diffuse Reflectance Infrared Spectroscopy. *Chem. Phys. Lett.* **2002**, *351*, 105–108.
- Kossovsky, N.; Gelman, A.; Hnatyszyn, H. J.; Rajguru, S.; Garrell, R. L.; Torbati, S.; Freitas, S. S. F.; Chow, G.-M. Surface-Modified Diamond Nanoparticles as Antigen Delivery Vehicles. *Bioconjugate Chem.* **1995**, *6*, 507–511.
- Gu, H.; Su, X. d.; Loh, K. P. Electrochemical Impedance Sensing of DNA Hybridization on Conducting Polymer Film-Modified Diamond. *J. Phys. Chem. B* **2005**, *109*, 13611–13618.
- Huang, T. S.; Tzeng, Y.; Liu, Y. K.; Chen, Y. C.; Walker, K. R.; Guntupalli, R.; Liu, C. Immobilization of Antibodies and Bacterial Binding on Nanodiamond and Carbon Nanotubes for Biosensor Applications. *Diam. Relat. Mater.* **2004**, *13*, 1098–1102.
- Huang, H.; Pierstorff, E.; Ōsawa, E.; Ho, D. Active Nanodiamond Hydrogels for Chemotherapeutic Delivery. *Nano Lett.* **2007**, *7*, 3305–3314.
- Huang, H.; Pierstorff, E.; Ōsawa, E.; Ho, D. Protein-Mediated Assembly of Nanodiamond Hydrogels into a Biocompatible and Biofunctional Multilayer Nanofilm. *ACS Nano* **2008**, *2*, 203–212.
- Dolmatov, V. Y. Detonation Synthesis Ultradispersed Diamonds: Properties and Applications. *Russ. Chem. Rev.* **2001**, *70*, 607–626.
- Schrand, A. M.; Huang, H.; Carlson, C.; Schlager, J. J.; Ōsawa, E.; Hussain, S. M.; Dai, L. Are Diamond Nanoparticles Cytotoxic? *J. Phys. Chem. B* **2007**, *111*, 2–7.
- Liu, K.-K.; Cheng, C.-L.; Chang, C.-C.; Chao, J.-I. Biocompatible and Detectable Carboxylated Nanodiamond on Human Cell. *Nanotechnology* **2007**, *18*, 325102.
- Yu, S.-J.; Kang, M.-W.; Chang, H.-C.; Chen, K.-M.; Yu, Y.-C. Bright Fluorescent Nanodiamonds: No Photobleaching and Low Cytotoxicity. *J. Am. Chem. Soc.* **2005**, *127*, 17604–17605.
- Härtl, A.; Schmich, E.; Garrido, J. A.; Hernando, J.; Catharino, S. C. R.; Walter, S.; Feulner, P.; Kromka, A.; Steinmüller, D.; Stutzmann, M. Protein-Modified Nanocrystalline Diamond Thin Films for Biosensor Applications. *Nat. Mater.* **2004**, *3*, 736–742.
- Yang, W.; Auciello, O.; Butler, J. E.; Cai, W.; Carlisle, J. A.; Gerbi, J. E.; Gruen, D. M.; Knickerbocker, T.; Lasseter, T. L.; Russell, J. N., Jr. DNA-Modified Nanocrystalline Diamond Thin-Films as Stable, Biologically Active Substrates. *Nat. Mater.* **2002**, *1*, 253–257.

31. Hahn, A. W.; York, D. H.; Nichols, M. F.; Amromin, G. C.; Yasuda, H. K. Biocompatibility of Glow-Discharge-Polymerized Films and Vacuum-Deposited Parylene. *J. Appl. Polym. Sci. Symp.* **1984**, *38*, 55–64.
32. Yamagishi, F. G. Investigation of Plasma-Polymerized Films as Primers for Parylene-C Coatings on Neural Prosthesis Materials. *Thin Solid Films* **1991**, *202*, 39–50.
33. Schmidt, E. M.; McIntosh, J. S.; Bak, M. J. Long-Term Implants of Parylene-C Coated Microelectrodes. *Med. Biol. Eng. Comput.* **1988**, *26*, 96–101.
34. Burkel, W. E.; Kahn, R. H. Cell-Lined, Nonwoven Microfiber Scaffolds as a Blood Interface. *Ann. N.Y. Acad. Sci.* **1977**, *283*, 419–437.
35. Fortin, J. B.; Lu, T.-M. A Model for the Chemical Vapor Deposition of Poly(*para*-xylylene) (Parylene) Thin Films. *Chem. Mater.* **2002**, *14*, 1945–1949.
36. Chang, T. Y.; Yadav, V. G.; Leo, S. D.; Mohedas, A.; Rajalingam, B.; Chen, C.-L.; Selvarasah, S.; Dokmeci, M. R.; Khademhosseini, A. Cell and Protein Compatibility of Parylene-C Surfaces. *Langmuir* **2007**, *23*, 11718–11725.
37. Jain, R. K. Delivery of Molecular and Cellular Medicine to Solid Tumors. *Adv. Drug Delivery Rev.* **2001**, *46*, 149–168.
38. Gorham, W. F. A New, General Synthetic Method for the Preparation of Linear Poly-*p*-xylylenes. *J. Polym. Sci., Part A* **1966**, *4*, 3027–3039.
39. Boduroglu, S.; Cetinkaya, M.; Dressick, W. J.; Singh, A.; Demirel, M. C. Controlling the Wettability and Adhesion of Nanostructured Poly-*p*-xylylene) Films. *Langmuir* **2007**, *23*, 11391–11395.
40. Lee, J. H.; Hwang, K. S.; Kim, T. S. Effect of Oxygen Plasma Treatment on Adhesion Improvement of Au Deposited on Pa-c Substrates. *J. Kor. Phys. Soc.* **2004**, *44*, 1177–1181.
41. Spellman, G. P.; Carley, J. F.; Lopez, L. A. Vacuum Deposition of Parylene Films: Influence of Process Factors and Baffling on Film Thickness Distribution. *J. Plast. Film Sheeting* **1999**, *15*, 308–328.
42. Robinson, E. M.; Lam, R.; Pierstorff, E. D.; Ho, D. Localized Therapeutic Elution via an Amine-Functionalized Poly-*p*-xylylene Microfilm Device. *J. Phys. Chem. B* **2008**, *112*, 11451–11455.
43. Huang, X.; Brazel, C. S. On the Importance and Mechanisms of Burst Release in Matrix-Controlled Drug Delivery Systems. *J. Controlled Release* **2001**, *73*, 121–136.
44. Tannock, I. F. Tumor Physiology and Drug Resistance. *Cancer Metastasis Rev.* **2001**, *20*, 123–132.
45. Lankelma, J.; Dekker, H.; Luque, R. F.; Luykx, S.; Hoekman, K.; van der Valk, P.; van Diest, P. J.; Pinedo, H. M. Doxorubicin Gradients in Human Breast Cancer. *Clin. Cancer Res.* **1999**, *5*, 1703–1707.
46. Tannock, I. F.; Lee, C. M.; Tunggal, J. K.; Cowan, D. S. M.; Egorin, M. J. Limited Penetration of Anticancer Drugs through Tumor Tissue: A Potential Cause of Resistance of Solid Tumors to Chemotherapy. *Clin. Cancer Res.* **2002**, *8*, 878–884.
47. Legha, S. S.; Benjamin, R. S.; Mackay, B.; Ewer, M.; Wallace, S.; Valdivieso, M.; Rasmussen, S. L.; Blumenschein, G. R.; Freireich, E. J. Reduction of Doxorubicin Cardiotoxicity by Prolonged Continuous Intravenous Infusion. *Ann. Intern. Med.* **1982**, *96*, 133–139.